Int J Clin Exp Med 2017;10(9):13526-13533
www.ijcem.com /ISSN:1940-5901/IJCEM0055256

Original Article

The value of CT image-based texture analysis for differentiating renal primary undifferentiated pleomorphic sarcoma from three subtypes of renal cell carcinoma

Guoshun Liu[1,2], Wenxi Li[3], Lei Li[4], Xinqing Jiang[2]

[1]The First Affiliated Hospital of Jinan University, Guangzhou, China; Departments of [2]Radiology, [3]Geriatrics, Guangzhou First People's Hospital, Guangzhou Medical University, Guangzhou, China; [4]Department of Radiology, 184 Hospital of The People's Liberation Army, Yingtan, China

Received December 14, 2016; Accepted August 7, 2017; Epub September 15, 2017; Published September 30, 2017

Abstract: Purpose: To explore the value of computed tomography (CT) image-based texture analysis for the differential diagnosis of renal primary undifferentiated pleomorphic sarcoma and three subtypes of renal cell carcinoma. Materials and methods: Eleven cases of renal primary undifferentiated pleomorphic sarcoma and 33 cases of renal cell carcinoma (including 11 cases each of clear cell carcinoma, papillary renal cell carcinoma, and chromophobe renal cell carcinoma), which were confirmed by surgical pathology, were retrospectively analyzed. All patients underwent an abdominal CT scan and a three-phase enhanced scan (except for 1 patient with undifferentiated polymorphic sarcoma without a delayed scan). MaZda software was used to manually place regions of interest (ROIs) to extract the textural features of the lesions. The texture feature selection methods included the Fisher coefficient, the joint error coefficient (POE+ACC), the mutual information (MI), and the above three methods combined (FPM). First, these 4 methods were used to select the most meaningful texture features for the identification of primary undifferentiated pleomorphic sarcoma and 3 subtypes of renal cell carcinoma. Then, raw data analysis (RDA), principal component analysis (PCA), and linear discriminant analysis (LDA) were used to identify the four types of lesions. The results are expressed as the misclassified rate (MCR). In addition, using the 4 selected categories, 2 intermediate or more senior doctors assessed and classified the imaging data of the 44 cases. Results: Based on the 4 phase CT images and the use of the Fisher, POE+ACC, MI, and FPM methods to extract texture features and RDA and PCA to identify the 44 cases, we found that the MCR was high (65.12-77.27%), and the misjudgement results showed no statistically significant differences ($P>0.05$). The MCR using LDA was low (6.82-59.09%) and showed a statistically significant difference from that resulting from the use of RDA and PCA ($P<0.05$). The lowest MCR was obtained with the FPM method using LDA and showed a statistically significant difference from those of the Fisher, POE+ACC, and MI methods. Based on the values obtained using the FPM method with LDA, no significant differences were found among the misdiagnoses in all of the phases ($x^2=3.526$, $P>0.05$). The MCR was lowest in the arterial phase (6.82%, 3/44). The MCR of the imaging diagnosis was 45.45% and showed a statistically significant difference from that obtained with the FPM method using LDA ($x^2=17.001$, $P<0.05$). Conclusion: The combined use of MaZda software, the FPM method to extract CT image texture features, and LDA produced the highest rate of identification of renal primary undifferentiated pleomorphic sarcoma and 3 subtypes of kidney cancer.

Keywords: Texture analysis, primary undifferentiated pleomorphic sarcoma, renal cancer carcinoma, subtype, differentiation

Introduction

Renal cell carcinoma (RCC) and primary undifferentiated pleomorphic sarcoma (PUPS) are the most common and rare renal neoplasms, respectively. Computed tomography (CT) and magnetic resonance imaging (MRI) examinations are more commonly used for the identification of common diseases [1-3], but the diagnosis of atypical and rare diseases is more experience-dependent and subjective. The imaging characteristics of different subtypes of renal cell carcinoma overlap. Primary undifferentiated pleomorphic sarcoma is clinically rare

and its imaging features lack specificity, which makes a clear diagnosis difficult [4, 5]. Texture analysis can provide information that cannot be seen by the naked eye via the quantitative analysis of the image pixel grey value of the local characteristics, the pixel value variation, and the distribution pattern. In recent years, this method has been applied to the medical imaging of many types of auxiliary diseases [6, 7]. At present, few studies on the application of image texture analysis in the kidney have been conducted. However, kidney cancer is one of the most common tumours. Different types of kidney cancer and renal primary undifferentiated pleomorphic sarcoma require different clinical treatments, and a correct diagnosis is helpful to form a reasonable treatment plan. Therefore, the aim of this study was to explore the value of CT image-based texture analysis for the differential diagnosis of renal primary undifferentiated pleomorphic sarcoma and 3 subtypes of renal cell carcinoma.

Patients and methods

Patients

This study was approved by the Institutional Review Board of Guangzhou First People's Hospital. The clinical investigations in this study were conducted according to the principles expressed in the Declaration of Helsinki. Informed consent, written or oral, was obtained from all of the participants. This retrospective study utilized de-identified patient data collected from the CT room in the Department of Radiology at Guangzhou First People's Hospital affiliated to Guangzhou Medical University. Eleven cases (all patients underwent a CT scan before surgery, 10 patients underwent a three-phase enhanced scan, and 1 patient underwent only arterial and venous phase scans) of PUPS of the kidney were diagnosed by surgery and pathology at Guangzhou First People's Hospital from December 2004 to August 2016. Seven of the patients were male and 4 were female, and their ages ranged from 38 to 76 years, with a mean age of 60±11 years. We analyzed 213 cases of renal cell carcinoma confirmed by surgical pathology from December 2004 to August 2016 at Guangzhou First People's Hospital, of which 11 cases each of clear cell carcinoma, papillary carcinoma, and chromophobe renal cell carcinoma were randomly selected (7 males and 4 females with clear cell carcinoma, age 27-81 years, average age 56±8 years; 5 males and 6 females with papillary carcinoma, age 23-73 years, average age 55±13 years; and 8 males and 3 females with chromophobe renal cell carcinoma, age 33-68 years, average age 45±13 years).

CT examination

All examinations were performed using a 16-MDCT (TOSHIBA Aquision, Japan) and included a plain scan and an enhanced scan with the following scanning parameters: collimator 0.625 mm, tube voltage 100-120 kV, tube current 120-160 mAs, layer thickness 5.0 mm, and layer spacing 3-5 mm. A non-ionic contrast agent (2 mL/kg, Ultravist 350, Bayer AG, Leverkusen, Germany) was administered, which was adjusted for the patient's weight in kg and automatically injected at a flow rate of 4 mL/s through the elbow vein with a double cylinder high pressure syringe. Approximately 25-30 s, 60-70 s, and 128-180 s after the contrast agent injection, the arterial phase, venous phase, and excretory phase were obtained, respectively.

Image texture analysis

Image selection

The CT images of all of the patients were exported from the PACS work station in a BMP format. The window width and window position were adjusted for consistency, and the data were stored on the hard disk for further analysis. The diagnosis of these 44 patients was performed by two intermediate or more superior physicians who had experience in the diagnosis of abdominal images. The diagnosis was based on a 4-by-1 rule: A represented clear cell carcinoma, B represented papillary renal cell carcinoma, C represented chromophobe renal cell carcinoma, and D represented undifferentiated pleomorphic sarcoma. A consensus was reached in the cases of disagreement regarding the diagnosis.

Texture analysis

Image texture feature extraction: A texture analysis was performed using MaZda software (Version 4.7, the Technical University of Lodz, Institute of Electronics, http://www.eletel.p.lodz.pl/mazda/). To reduce the error of the region of interest (ROI) of the different

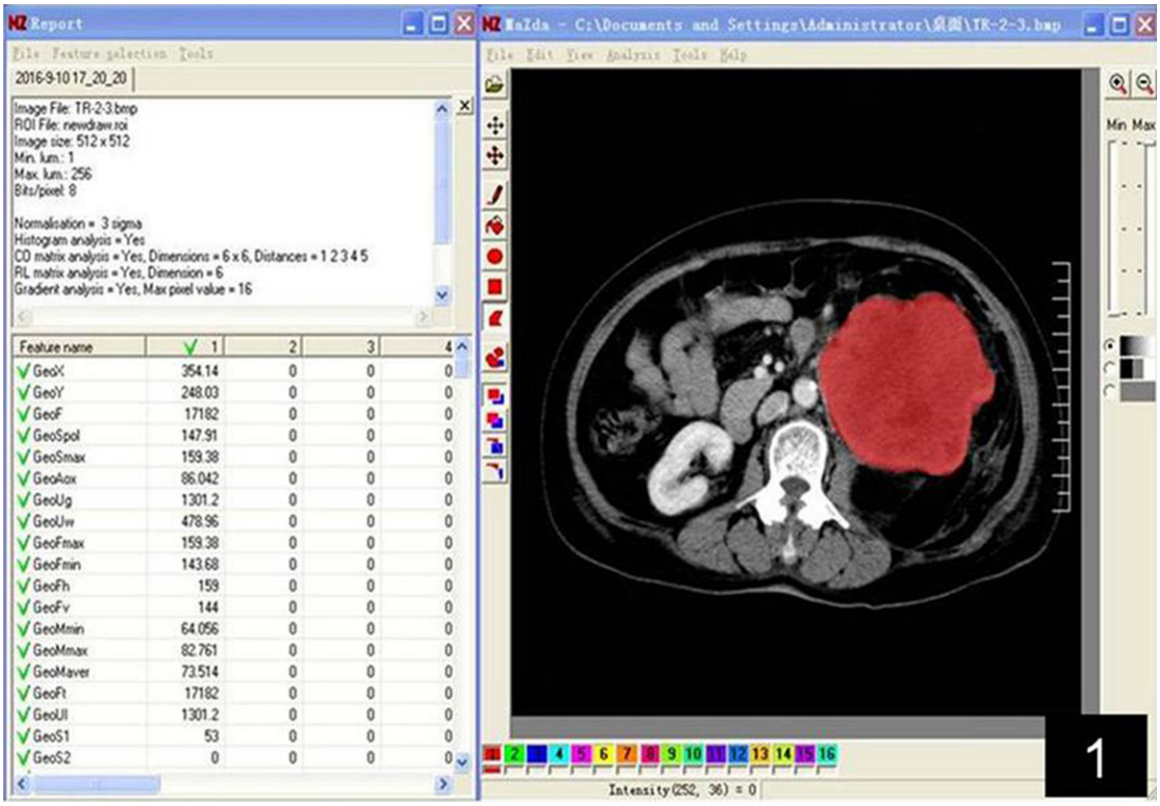

Figure 1. Manually drawn ROI at the maximum level in the clearest phase.

Table 1. Texture feature parameters generated by the MaZda software

Texture description	Texture feature parameters
Histogram	Mean, variance, skewness, kurtosis, percentile value
Greylevelco-occurrence matrix	ASM energy, contrast, autocorrelation, entropy, entropy sum, square sum, variance and inverse moment, entropy difference
Run-length check	Non-uniformity measure of run length, non-uniformity measure of grey scale, long run enhancement, short run enhancement, fractional run
Absolute gradient	Gradient mean, variance, skewness, kurtosis, non-zero
Autoregressive model	Theta 1-4, sigma
Wavelet transform	The energy of the wavelet transform coefficients in each band (3 subsampling factors)

phases, the boundary of the ROI at the maximum level in the clearest phase was manually drawn while maintaining consistency with the other phases (**Figure 1**). The grey level co-occurrence matrix (GLCM), grey histogram, run-length matrix (RUN), texture features based on a Fourier transform, and auto-regressive method were generated after the texture features were normalized to reduce the effects of contrast and brightness changes (**Table 1**). Due to the number of texture features, we selected the most discriminating features of these two types of lesions for further analysis. The MaZda software provides the Fisher coefficient (Fisher), classification error probability combined with the average correlation coefficients (POE+ACC), mutual information (MI) of the three types of methods with the 10 most significant texture feature selections, and the combination of the 3 methods (FPM) with the 30 most significant texture feature selections for further analysis of the disease classification.

Discriminate analysis: The selected texture features were used to classify 4 types of lesions using B11 statistical software (version 4.7, the Technical University of Lodz, Institute of Electronics, http://www.eletel.p.lodz.pl/mazda/). The discriminate methods include draw data analysis (RDA), principal component analysis (PCA),

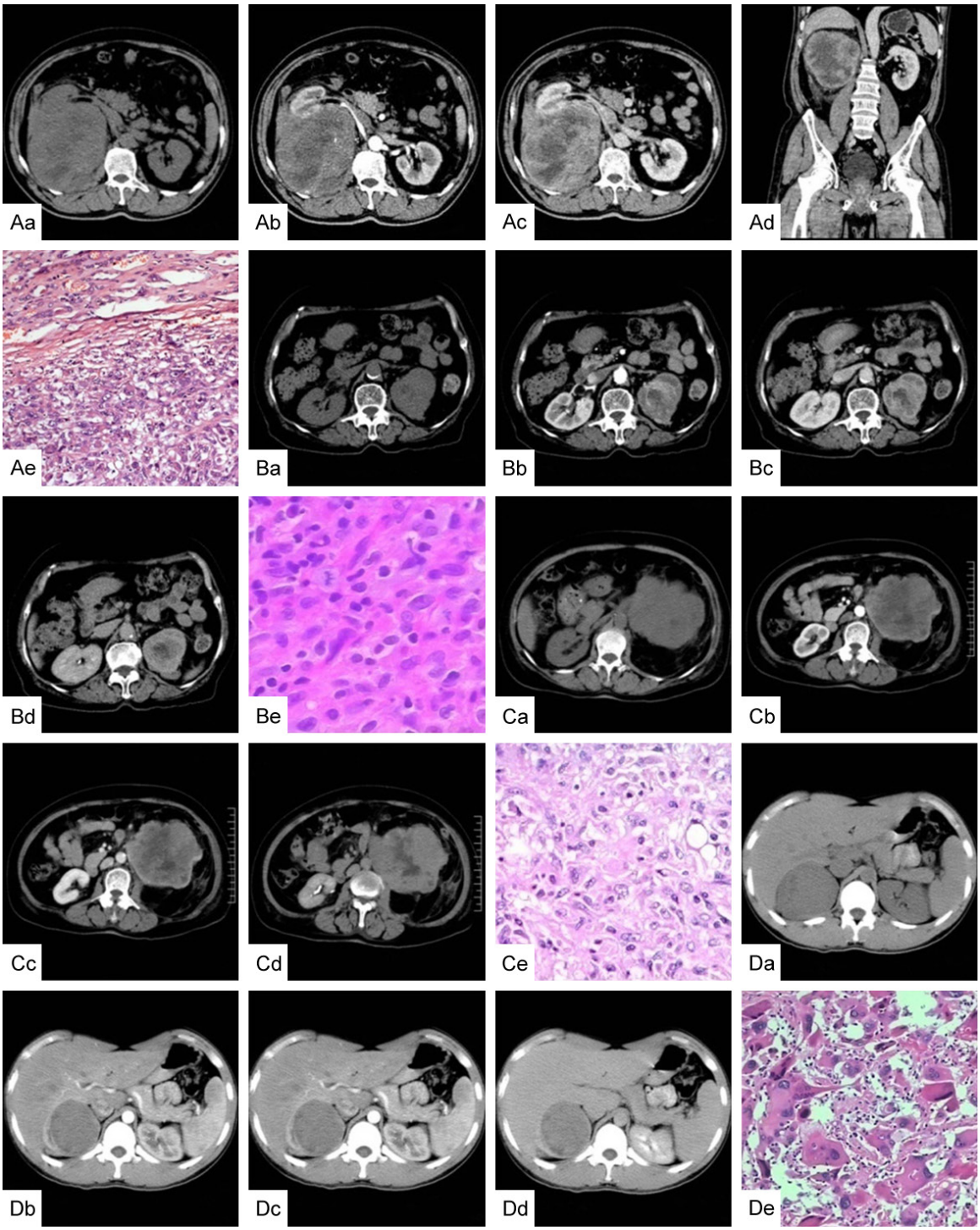

Figure 2. Aa-d. A 65-year-old male with renal primary undifferentiated pleomorphic sarcoma was correctly diagnosed. The CT enhanced scan shows moderate progressive enhancement, larger lesions, cystic necrosis, and more violations of the perirenal space. Ba-d. A 47-year-old female with renal primary undifferentiated pleomorphic sarcoma was misdiagnosed with clear cell carcinoma. The CT enhanced scan shows moderately fast-forward and fast-out enhancement, a smaller lesion volume, less necrosis, and no perirenal invasion. Ca-d. A 56-year-old male with renal primary undifferentiated pleomorphic sarcoma was misdiagnosed with chromophobe renal cell carcinoma. The CT enhanced scan shows mild progressive enhancement, a centrally segmentally located, low-density enhancement zone with a narrow time delay range, no significant renal involvement, and perirenal fascia thickening (due to chronic stimulation). Da-d. A 33-year-old male with renal primary undifferentiated pleomorphic sarcoma was misdiagnosed with papillary carcinoma. No significant enhancement of the CT scans in any stage, no obvious necrosis, a smaller lesion volume, and no perirenal invasion were observed. Ae, Be, Ce, and De. Show the corresponding

pathological maps. The pleomorphic morphology of the tumour cells, which were mostly irregular or round in shape, was obvious. Red dye staining showed increased megakaryocytes, multinucleated tumour cells, the nucleus, obvious nucleoli with a pathological split phase, increased mixed foam-like cells, lymphocytes and plasma cells, and local tissue necrosis.

Table 2. Identification of renal primary undifferentiated pleomorphic sarcoma and 3 subtypes of renal cell carcinoma

Phase	Method of texture extraction	Method of discriminant analysis		
		RDA	PCA	LDA
Plain phase	Fisher	34/44	34/44	26/44
	POE+ACC	34/44	34/44	26/44
	MI	34/44	34/44	26/44
	FPM	33/44	34/44	9/44
Arterial phase	Fisher	30/44	30/44	18/44
	POE+ACC	30/44	30/44	18/44
	MI	30/44	30/44	18/44
	FPM	30/44	29/44	3/44
Venous phase	Fisher	29/44	30/44	15/44
	POE+ACC	29/44	30/44	15/44
	MI	29/44	30/44	15/44
	FPM	31/44	31/44	6/44
Delay phase	Fisher	28/43	28/43	23/43
	POE+ACC	28/43	28/43	23/43
	MI	28/43	28/43	23/43
	FPM	29/43	29/43	7/43

Fisher: Fisher coefficient. POE+ACC: classification error probability combined with the average correlation coefficients. MI: mutual information. FPM: Fisher+POE+ACC+MI. RDA: raw data analysis. PCA: principal component. LDA: linear discriminant analysis.

and linear discriminate analysis (LDA). The results obtained in the 4 different phases of lesions were expressed as the misclassified rate (MCR=number of misclassified cases/total number of cases × 100%), and a lower MCR indicated that the lesion contains more texture features.

Statistical analysis

Using the pathology as the reference standard, Linex List data x^2 test was used to examine the differences in the results for the different phases, texture extractions, and analysis methods and to determine whether a statistically significant difference was present between the diagnoses provided by the physicians according to the images and the MaZda software. The statistical analyses were performed using SPSS version 13.0. A P value <0.05 was considered significant.

Results

Diagnoses of physicians based on CT images

Of the 11 cases of renal PUPS, 4 cases were diagnosed correctly (**Figure 2**), and 7 cases were misdiagnosed as renal cell carcinoma (4 cases were misdiagnosed as clear cell carcinoma, as shown in **Figure 2B**; 2 cases were misdiagnosed aschromophobe renal cell carcinoma, as shown in **Figure 2C**; and 1 case was misdiagnosed as papillary cell carcinoma, as shown in **Figure 2D**. Of the 11 cases of renal clear cell carcinoma, 9 cases were diagnosed correctly (1 case was misdiagnosed as chromophobe renal cell carcinoma and 1 case was misdiagnosed as papillary cell carcinoma). Of the 11 cases of renal chromophobe renal cell carcinoma, 7 cases were diagnosed correctly (3 cases were misdiagnosed as clear cell carcinoma and 1 case was misdiagnosed as papillary cell carcinoma). Of the 11 cases of renal papillary cell carcinoma, 4 cases were diagnosed correctly (5 cases were misdiagnosed as clear cell carcinoma and 2 cases were misdiagnosed as chromophobe renal cell carcinoma). Of the 44 cases, 24 cases were diagnosed correctly and 20 cases were misdiagnosed, resulting in an MCR of 45.45% (20/44).

The statistical analysis of the MCR and the misjudged difference based on CT image texture analysis

As shown in **Table 2**, used Linex List data x^2 test, we found that based on the 4 methods used to extract the texture features (Fisher, POE+ACC, MI, and FPM), regardless of the use of plain scans, the arterial phase, the venous phase, or the delay period, the MCR using LDA was relatively lower than that of RDA and PCA, and the FPM texture extraction method using LDA produced the lowest value. The misjudged results of RDA and PCA showed no significant differences in all of the phases (P>0.05), and the MCR was high (65.12%-77.27%). Based on CT plain and delay scan image, whether to use

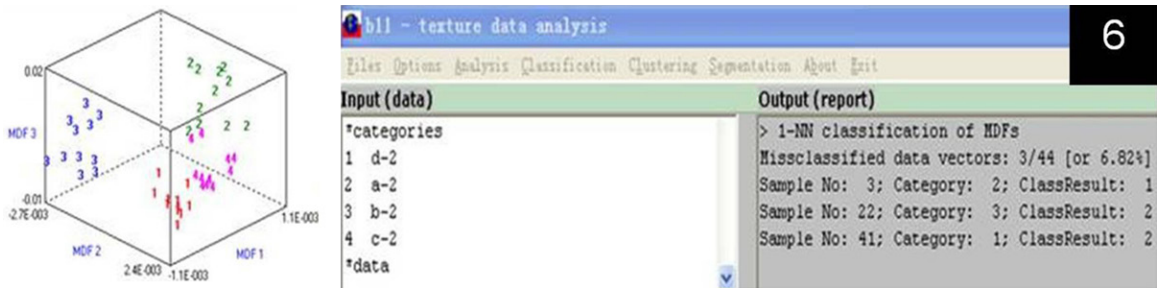

Figure 3. Differential diagnosis of renal primary undifferentiated pleomorphic sarcoma and 3 subtypes of renal cell carcinoma based on the FPM method using LDA in the arterial phase. The number 1 represents undifferentiated pleomorphic sarcoma, 2 represents chromophobe renal cell carcinoma, 3 represents clear cell carcinoma, and 4 represents papillary renal cell carcinoma. The four types of lesions were more dispersed in different regions, which made them easier to distinguish. Three cases were misjudged, including 1 case of undifferentiated pleomorphic sarcoma that was misdiagnosed as chromophobe renal cell carcinoma, 1 case of chromophobe renal cell carcinoma that was misdiagnosed as undifferentiated pleomorphic sarcoma, and 1 case of clear cell carcinoma that was misdiagnosed as chromophobe renal cell carcinoma.

Table 3. Differentiation of primary undifferentiated pleomorphic sarcoma and 3 subtypes of renal cell carcinoma according to LDA and image-based physician diagnoses

Identification method	Incorrect diagnoses	Correct diagnoses
LDA	3	41
Image-based physician diagnoses	20	24
	x^2=17.001	P=0.000

Statistical difference using the FPM method and LDA based on CT arterial phase images and physician diagnoses (P<0.01).

Fisher, POE+ACC or MI texture extraction method, the misdiagnosis results of using LDA showed no significant differences with RDA and PCA (P>0.05), but based on CT arterial phase and venous phase image, the misdiagnosis results of using LDA showed a statistically significant differences with RDA and PCA (P<0.05). A statistically significant difference was found between the FPM method using LDA and RDA and PCA (P<0.05). Based on the FPM method using LDA, no significant difference was observed in the misdiagnosis results in all of the phases (x^2=3.526, P>0.05), and the MCR exhibited the lowest value in the arterial phase (6.82%, 3/44). Based on the FPM method using LDA, 3 cases were misdiagnosed, including 1 case of undifferentiated pleomorphic sarcoma that was misdiagnosed as chromophobe renal cell carcinoma, 1 case of chromophobe renal cell carcinoma that was misdiagnosed as undifferentiated pleomorphic sarcoma, and 1 case of clear cell carcinoma that was misdiagnosed as chromophobe renal cell carcinoma (**Figure 3**).

Statistical analysis of the misjudged difference using the FPM method and LDA based on CT arterial phase images and physician diagnoses

As shown in **Table 3**, used 2 × 2 data x^2 test we found a statistically significant difference between the two methods (x^2=17.001, P<0.05).

Discussion

Differentiation of renal primary undifferentiated pleomorphic sarcoma and 3 subtypes of renal cell carcinoma based on CT images

Clinically, CT scans are often used in imaging examinations of kidney disease, which exhibit good application value [8]. However, the results of CT imaging examinations are limited by the level of diagnosis and depend on the experience and subjectivity of the physician, especially in the case of rare and atypical diseases. Renal carcinoma is the most common malignant neoplasm of the kidney. Its imaging manifestations have a certain specificity, which facilitates diagnosis. However, its subtypes are diverse, and by relying solely on CT imaging, it is difficult to distinguish the subtypes [9]. Clear cell carcinoma, papillary carcinoma, and chromophobe renal cell carcinomaare the most common subtypes of renal cell carcinoma, and although the imaging findings have certain

characteristics, some overlap occurs [10]. Radiologists mainly rely on the distinctive characteristics for diagnosis, which can significantly increase the MCR. The diagnostic accuracy of these diseases obtained in this study was 60.61% (20/33). Primary undifferentiated pleomorphic sarcoma is a rare malignant tumour of the kidney, and its imaging features lack specificity. Imaging diagnosis is difficult and this type of tumour is easy to misdiagnose; thus, the diagnostic accuracy in this study was only 36.36% (4/11). Therefore, based on CT images, it is very difficult to differentiate between renal primary undifferentiated polymorphic sarcoma and the 3 subtypes of renal cell carcinoma.

Differentiation of renal primary undifferentiated pleomorphic sarcoma and 3 subtypes of renal cell carcinoma based on CT image texture analysis

Texture analysis utilizes the changes in the grey value of image pixels and their distribution pattern, which can reflect microscopic pathological changes that are not visible and can be used in the analysis of various images [11]. MaZda, a software package for 2D and 3D image texture analysis, provides a complete path for the quantitative analysis of image textures [12]. MaZda software provides 4 methods of texture extraction: Fisher, POE+ACC, MI, and FPM [13]. The first three methods automatically select the 10 most significant features of the lesions, whereas the FPM method selects the 30 most significant texture features [14]. Compared to the previous 3 methods, which provide more texture features, the prediction accuracy of the FPM method is relatively high, as confirmed by this study. In addition, MaZda software provides 2 categories of discriminant classification methods, including linear classification (RDA, PCA, and LDA) and nonlinear classification (NDA) [15]. Because the data obtained in this study are not subject to nonlinear classification, only linear classification was performed. The results showed significant differences between the FPM using LDA and RDA/PCA, with a significantly lower MCR for the FPM than for RDA/PCA. Based on the FPM texture extraction of LDA, a significant difference was not observed for misclassifications between all of the phases, and the MCR of the arterial phase exhibited the lowest value (6.82%, 3/44). We also found significant differences between the results of the FPM using LDA and the diagnoses of physicians using imaging methods for renal primary undifferentiated pleomorphic sarcoma and the 3 subtypes of kidney cancer, with a significantly lower MCR for the FPM using LDA than for the imaging diagnosis (52.27%, 20/44). Thus, the FPM texture extraction of LDA, which can successfully identify primary renal undifferentiated pleomorphic sarcoma and the 3 subtypes of renal cancer, was significantly better than conventional imaging diagnosis, with the highest anastomosis (93.18%, 41/44) in the arterial phase, which is consistent with that of conventional CT-enhanced arterial phase images that provide more imaging information.

Limitations

The limitations of this study are as follows. First, due to the low incidence of undifferentiated pleomorphic sarcoma of the kidney, the number of cases in this study was low. We hope to further expand the number of cases in follow-up studies. Second, this study is a retrospective study. In follow-up studies, we hope to establish the discriminant equation by expanding the sample to conduct a prospective analysis. Third, this study is based on a single CT image texture feature extraction. The ideal situation would involve 3D modelling of the CT image sequence and determining the texture characteristics of lesions using 3D spatial analyses [16].

In summary, the combination of MaZda software, the combined method (FPM) of extracting CT image texture features, and the linear classification analysis (LDA) can be used to differentiate renal primary undifferentiated pleomorphic sarcoma and 3 subtypes of kidney cancer. Therefore, texture analysis-based CT imaging can potentially be used as a clinical method for the differential diagnosis of atypical manifestations of common and rare kidney diseases.

Disclosure of conflict of interest

None.

Address correspondence to: Dr. Xinqing Jiang, Department of Radiology, Guangzhou First People's Hospital, Guangzhou Medical University, Panfu Road No 1, Guangzhou 510180, China. E-mail: 464330471@qq.com

References

[1] Bata P, Gyebnar J, Tarnoki DL, Tarnoki AD, Kekesi D, Szendroi A, Fejer B, Szasz AM, Nyirady P, Karlinger K and Berczi V. Clear cell renal cell carcinoma and papillary renal cell carcinoma: differentiation of distinct histological types with multiphase CT. DiagnInterv Radiol 2013; 19: 387-392.

[2] Yu X, Lin M, Ouyang H, Zhou C and Zhang H. Application of ADC measurement in characterization of renal cell carcinomas with different pathological types and grades by 3.0T diffusion-weighted MRI. Eur J Radiol 2012; 81: 3061-3066.

[3] Göğüş Ç, Gökce Mİ, Süer E, Tulunay Ö and Şafak M. Primary malignant fibrous histiocytoma of the kidney: report of a case and literature review. Turk J Urol 2013; 39: 194-197.

[4] Xue LY, Lu Q, Huang BJ, Li Z, Li CX, Wen JX and Wang WP. Papillary renal cell carcinoma and clear cell renal cell carcinoma: differentiation of distinct histological types with contrast-enhanced ultrasonography. Eur J Radiol 2015; 84: 1849-1856.

[5] Pathrose G, John NT and Manojkumar R. A rare case of malignant fibrous histiocytoma/pleomorphic undifferentiated sarcoma of the kidney. J Clin Diagn Res 2015; 9: PD27-PD29.

[6] Yoon SH, Kim YH, Lee YJ, Park J, Kim JW, Lee HS and Kim B. Tumor heterogeneity in human epidermal growth factor receptor 2 (HER2)-positive advanced gastric cancer assessed by CT texture analysis: association with survival after trastuzumab treatment. PLoS One 2016; 11: e0161278.

[7] Mougiakakou SG, Valavanis IK, Nikita A and Nikita KS. Differential diagnosis of CT focal liver lesions using texture features, feature selection and ensemble driven classifiers. ArtifIntell Med 2007; 41: 25-37.

[8] Kim SH, Kim CS, Kim MJ, Cho JY and Cho SH. Differentiation of Clear cell renal cell carcinoma from other subtypes and fat-poor angiomyolipoma by use of quantitative enhancement measurement during three-phase MDCT. AJR Am J Roentgenol 2016; 206: W21-W28.

[9] Ren A, Cai F, Shang YN, Ma ES, Huang ZG, Wang W, Lu Y and Zhang XZ. Differentiation of renal oncocytoma and renal clear cell carcinoma using relative CT enhancement ratio. Chin Med J (Engl) 2015; 128: 175-179.

[10] Ruppert-Kohlmayr AJ, Uggowitzer M, Meissnitzer T and Ruppert G. Differentiation of renal clear cell carcinoma and renal papillary carcinoma using quantitative CT enhancement parameters. AJR Am J Roentgenol 2004; 183: 1387-1391.

[11] Drabycz S, Roldán G, de Robles P, Adler D, McIntyre JB, Magliocco AM, Cairncross JG and Mitchell JR. An analysis of image texture, tumor location, and MGMT promoter methylation in glioblastoma using magnetic resonance imaging. NeuroImage 2010; 49: 1398-1405.

[12] Orphanidou-Vlachou E, Vlachos N, Davies NP, Arvanitis TN, Grundy RG and Peet AC. Texture analysis of T1-and T2-weighted MR images and use of probabilistic neural network to discriminate posterior fossa tumours in children. NMR Biomed 2014; 27: 632-639.

[13] Szczypiński PM, Strzelecki M, Materka A, Klepaczko A. MaZda--a software package for image texture analysis. Comput Methods Programs Biomed 2009; 94: 66-76.

[14] Gentillon H, Stefańczyk L, Strzelecki M and Respondek-Liberska M. Parameter set for computer-assisted texture analysis of fetal brain. BMC Res Notes 2016; 9: 496.

[15] Yan L, Liu Z, Wang G, Huang Y, Liu Y, Yu Y and Liang C. Angiomyolipoma with minimal fat: differentiation from clear cell renal cell carcinoma and papillary renal cell carcinoma by texture analysis on CT images. Acad Radiol 2015; 22: 1115-1121.

[16] De Albuquerque M, Anjos LG, Maia Tavares de Andrade H, De Oliveira MS, Castellano G, Junqueira Ribeiro de Rezende T, Nucci A and FrançaJunior MC. MRI texture analysis reveals deep gray nuclei damage in amyotrophic lateral sclerosis. J Neuroimaging 2016; 26: 201-206.